

CH₃NH₃Sn_xPb_{1-x}Br₃ hybrid perovskite solid solution: synthesis, structure and optical properties

Alessandro Mancini,^a Paolo Quadrelli,^a Chiara Milanese,^a Maddalena Patrini,^b Giorgio Guizzetti,^b and Lorenzo Malavasi^{a,*}

^aUniversity of Pavia and INSTM, Viale Taramelli 16, 27100 Pavia, Italy; ^bUniversity of Pavia and CNISM, Via Bassi 6, 27100 Pavia, Italy.

Supporting Information Placeholder

ABSTRACT: We report the synthesis and characterization of the MASn_xPb_{1-x}Br₃ (MA=methylammonium, nominal x=0, 0.2, 0.4, 0.5, 0.6, 0.8, 1) solid solution. The original synthetic method developed allowed to obtain single-phase materials with homogenous Sn/Pb distribution. All the samples prepared are cubic and the unit cell linearly reduces by increasing the x value. The optical response indicates a linear trend (Vegard's law) of the band gap by increasing the Sn-content moving from 2.20 eV (x=0) to 1.33 eV (x=1), thus extending the light absorption into the near-infrared.

The replacement of Pb with environmental friendly metals in organohalide perovskites for photovoltaics applications seems to be a required step in order to develop this promising technology. In addition, further modulation of the absorption spectrum (in particular towards the IR) is of interest for the implementation of organohalide perovskites in devices such as tandem cells.

Tin represents an excellent candidate element for lead replacement even though the problems related to Sn²⁺ oxidation by air should be considered in device design. However, Sn²⁺ has an ionic radius very close to that of Pb²⁺, thus making possible a complete solubility at the perovskite B-site with small lattice distortions.

Currently, very few examples of Pb-Sn systems have been reported in the literature. Hao et al.,¹ described the CH₃NH₃Sn_xPb_{1-x}I₃ (in the following CH₃NH₃=MA) system showing a non-linear trend in the energy band gap between the two end members. On the other hand, the same system, investigated later by Ogomi and co-workers², revealed a linear trend of the energy band gap by varying the x value. A detailed computational study of the mixed Sn-Pb MASn_xPb_{1-x}I₃ perovskites indicated a continuous and monotonic variation of the energy levels with the band gap energies shifting towards the near-IR spectral region as the Sn content in the perovskite increases.³ These computational results are in very good agreement with the experimental data reported in ref. 2. Finally, solar cells made with the MASn_xPb_{1-x}X₃ (X=I and Cl) perovskites were studied by Zuo et al., confirming an increased performance through broadened absorption and improved solution-cast film morphology due to the morphological modulation offered by Sn²⁺ incorporation. However, in

this paper the determination of the band gap of the mixed compositions was found to be challenging due to the ease of Sn oxidation.⁴

In view of the consideration reported above, it is clear that there is an urgent need of organohalide perovskites where Pb is replaced by environmental-friendly metals such as Sn and, in addition, to extend the series of mixed Pb/Sn perovskites reported so far. In this Letter we report the synthesis and the characterization of the MASn_xPb_{1-x}Br₃ system.

Samples of general formula MASn_xPb_{1-x}Br₃ (MA=methylammonium, x=0, 0.2, 0.4, 0.5, 0.6, 0.8, 1) were synthesized according to a general and original procedure we developed. In a typical synthesis, a proper stoichiometric amount of Pb acetate and tin bromide (sum of them resulting in 0.076 mol of metal precursors) are dissolved in an HBr excess (0.089 mol) under continuous mechanical stirring under nitrogen atmosphere. About 0.03 mol of hypophosphoric acid are added to the solution and inert atmosphere is maintained in the reaction environment in order to prevent Sn oxidation. Then, the solution is heated to 100°C and the corresponding amine solution (40%wt in water) is added in equimolar amount. The solution is then cooled down to 46°C at 1°C/min, until the formation of a precipitate, which is immediately filtered and dried under vacuum overnight. All the reagents were purchased from Sigma Aldrich in pure form and were used without any further purification. The crystal structure of the samples has been characterized by room temperature Cu-radiation X-ray Powder Diffraction (XRD) acquired with a Bruker D8 diffractometer. The optical diffuse reflectance spectra of the different perovskites were measured from 0.8 to 4.5 eV (250-1500 nm, with steps of 1 nm) by a Varian Cary 6000i equipped with an integrating sphere. For this kind of measurements polycrystalline powders were compacted into pellets of about 5 mm in diameter and reflectance spectra were calibrated using a standard reference disk. The elemental composition of the samples was determined by Energy-dispersive X-ray spectroscopy using an INCA Energy 350 X Max detector from Oxford Instruments linked to an EvoMA10 (Zeiss, Germany) scanning electron. Cobalt standard was used for the calibration of the quantitative elementary analysis. All the samples manipulations were carried out under inert atmosphere.

First of all, since we are dealing with a solid-solution, it is mandatory to check the actual stoichiometry of the samples with respect to the nominal composition and to explore the homogenous distribution of Sn and Pb in the material. For this reason, all the synthesized samples underwent careful elemental analysis by means of EDX. Table 1 reports the nominal and experimental (determined by EDX) x -values. Standard deviation in the analysis was $\pm 5\%$. Element mapping confirmed the homogeneous Sn/Pb distribution in all the samples.

Nominal x -value	Experimental x -value	a (Å)	E_g (eV)
0	0	5.9303(2)	2.20
0.20	0.09	5.9274(2)	2.00
0.40	0.23	5.9249(3)	1.93
0.50	0.34	5.9232(3)	
0.60	0.41	5.9211(3)	1.86
0.8	0.67	5.9137(4)	1.75
1	1	5.9082(4)	1.33

Table 1. Nominal and experimental x -values for the $\text{MASn}_x\text{Pb}_{1-x}\text{Br}_3$ system together with the a lattice constant determined from XRD and the E_g value.

As it can be appreciated from Table 1, all the mixed Sn/Pb samples show an actual Sn-content lower than the nominal one. Therefore, in the following discussion, we are going to use the experimental determined stoichiometries.

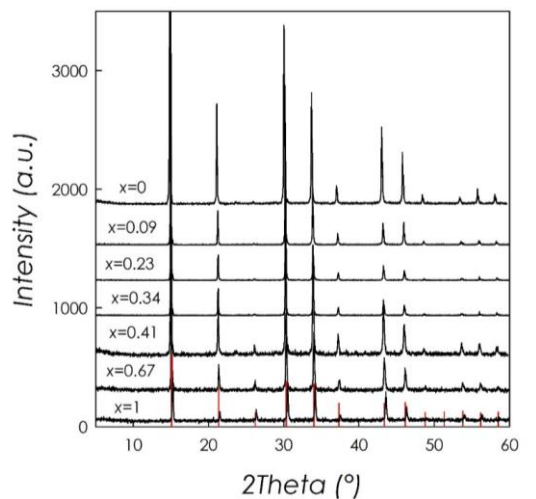


Figure 1. XRD patterns for the $\text{MASn}_x\text{Pb}_{1-x}\text{Br}_3$ solid solution (see Table 1). Vertical red bars refer to the reference structure for the MAPbBr_3 .

All the samples synthesized are single phase according to the XRD patterns. Phase analysis was carried out with the published crystal structures of the two end members which are both cubic (space group $Pm\bar{3}m$)^{5,6}. This unit cell has been found to properly describe the XRD patterns for all the members of the solid solution. The trend of the cubic lattice parameter obtained from the Rietveld refinement of the XRD patterns is reported in Figure 2 while the values are reported in Table 1.

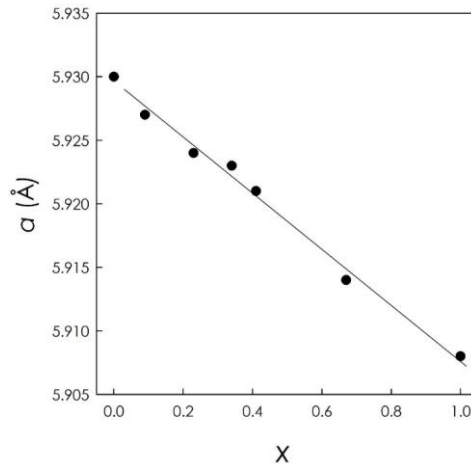


Figure 2. Cubic a lattice parameter vs. x for the $\text{MASn}_x\text{Pb}_{1-x}\text{Br}_3$ solid solution.

According to the plot of Figure 2, the $\text{MASn}_x\text{Pb}_{1-x}\text{Br}_3$ solid solution follows the Vegard's law with a progressive reduction of the lattice parameter by increasing the amount of Sn^{2+} ion due to its smaller ionic radius (1.35 Å) with respect to that of Pb^{2+} (1.49 Å)⁷. A continuous solid solution between the two end members (MAPbBr_3 and MASnBr_3) is then confirmed. A similar trend was not observed in the $\text{MASn}_x\text{Pb}_{1-x}\text{I}_3$ systems reported in ref. 1, most probably due to a poor control of samples stoichiometry and/or Sn oxidation state.

Figure 3 reports the vis-NIR diffuse reflectance spectra obtained on the samples considered in the present work. The positions of optical absorption edges, as determined from the extrapolation^{8,9} of the linear part of $[\text{F(R)} \text{h}\nu]^2$ where F(R) is the Kubelka-Munk function $\text{F(R)} = (1-\text{R})^2/2\text{R}$, are reported in Table 1.

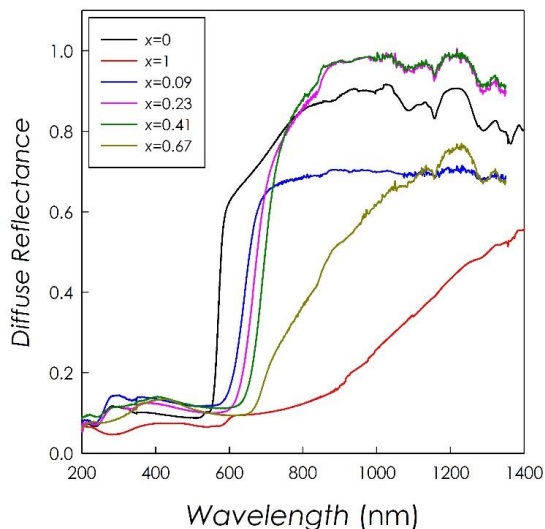


Figure 3. Diffuse reflectance spectra for the $\text{MASn}_x\text{Pb}_{1-x}\text{Br}_3$ solid solution.

From Figure 3 it is possible to note a progressive shift of the absorption spectrum at longer wavelengths as the Sn amount increases in the samples. In addition, the shape of the absorbance spectrum becomes broader as the x value increases. The band gap moves from 2.20 eV in MAPbBr_3 (a value in accordance with literature¹⁰) to about 1.33 eV in MASnBr_3 . The absorbance spectrum covered by

the samples reported here is not covered by Pb hybrid perovskites and such a sensitivity in the area of NIR spectral region is useful for all-solid-type tandem cells.

Figure 4 reports the trend of energy gap E_g as a function of Sn content (x) for the $\text{MASn}_x\text{Pb}_{1-x}\text{Br}_3$ solid solution (red circles).

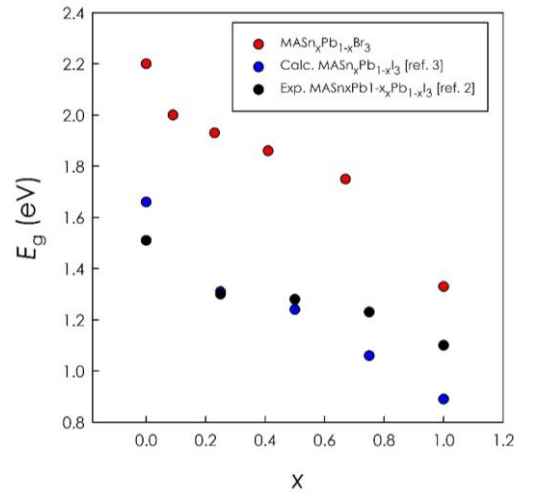


Figure 4. Trend of energy gap E_g as a function of the Sn content for the reflectance spectra for the $\text{MASn}_x\text{Pb}_{1-x}\text{Br}_3$ solid solution (red circles). Black circles are the values for the $\text{MASn}_x\text{Pb}_{1-x}\text{I}_3$ solid solution taken from ref. 2, while blue circles are the SOC-GW calculated values for the $\text{MASn}_x\text{Pb}_{1-x}\text{I}_3$ solid solution taken from ref. 3

In Figure 4 we compared the experimental values for the band gap of the $\text{MASn}_x\text{Pb}_{1-x}\text{Br}_3$ system determined in the present work together with the experimental values extracted from the experimental investigation of the $\text{MASn}_x\text{Pb}_{1-x}\text{I}_3$ solid solution of ref. 2 (black circles) and the calculated values for the $\text{MASn}_x\text{Pb}_{1-x}\text{I}_3$ system reported in ref. 3 (blue circles). In particular, the plotted calculated values from ref. 3 are those from the SOC-GW theory with optimized atomic and cell parameters.³

First of all, we note that our data for the $\text{MASn}_x\text{Pb}_{1-x}\text{Br}_3$ solid solution show a continuous and linear reduction of the band gap as the Sn content increases. With respect to the experimental data for the $\text{MASn}_x\text{Pb}_{1-x}\text{I}_3$ system² there is a different slope in the variation of the E_g , in particular for the data above $x=0.50$. On the other hand, the calculated and optimized values reported by Mosconi et al. for the I-based system, show a very similar trend in the reduction of the band gap value with the Sn-content with respect to the actual data we report for the Br-system. In addition, the comparison of the experimental band gap values for the $\text{MASn}_x\text{Pb}_{1-x}\text{Br}_3$ solid solution and the calculated values for the $\text{MASn}_x\text{Pb}_{1-x}\text{I}_3$ system highlights a quite rigid shift of the order of 0.5-0.6 eV which has been found as the constant difference in MAPbX_3 system passing from I to Br anion.¹¹ Such results are in agreement with the nature of the calculated band-structure of the Sn/Pb mixed systems.³

The difference in the experimental band gap trend with the Sn content between the $\text{MASn}_x\text{Pb}_{1-x}\text{X}_3$ solid solutions ($\text{X}=\text{Br}$ and I) could be due to a partial oxidation of the Sn in the samples with higher x -values reported in ref. 2, as indicated by the Authors. In the present case much care has been made in order to avoid any oxygen contamination and the XRD patterns of the sample before and after the optical measurements were found to be superimposable. The

data reported here further confirm the linear reduction of the band gap with Sn-content increase in the $\text{MASn}_x\text{Pb}_{1-x}\text{X}_3$ systems thus raising some doubts on the quality of the samples and data reported in ref. 1.

CONCLUSIONS

In the present paper we reported, for the first time, the synthesis and characterization of the $\text{MASn}_x\text{Pb}_{1-x}\text{Br}_3$ solid solution for nominal $x=0, 0.2, 0.4, 0.5, 0.6, 0.8, 1$.

XRD data confirmed the formation of single-phase materials with cubic symmetry for all the compositions with a linear reduction of the unit cell by increasing the Sn content (in accordance with the Vegard's law) and confirming the formation of a complete solid solution between the end members. EDX analysis showed that, with the synthetic method employed here, the final Sn stoichiometries are smaller than the nominal ones. Optical data revealed a progressive red shift of the absorption spectrum along with the increase of the Sn content and a broadening of the absorption edge. The band gap calculated from the diffuse reflectance spectra shows a linear reduction by increasing x shifting from 2.20 eV in MAPbBr_3 to about 1.33 eV in MASnBr_3 . The trend of the band gap variation with Sn-content is in partial agreement with previously reported experimental data for the $\text{MASn}_x\text{Pb}_{1-x}\text{I}_3$ solid solution and in very good agreement with calculated values for the same system.

The present results provide a new series of organohalide perovskites with reduced amount of Pb (or Pb-free) and with a range of optical band gap moving towards the near IR spectral region where hybrid organic-inorganic perovskites are sought in order to design all-solid-state tandem cells.

AUTHOR INFORMATION

Corresponding Author

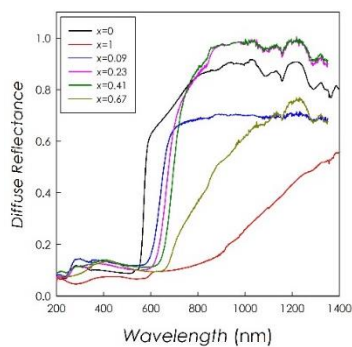
E-mail: lorenzo.malavasi@unipv.it

ACKNOWLEDGMENT

Financial support by University of Pavia and MIUR (PRIN 2011, CUP: F11J12000210001) is gratefully acknowledged. PQ warmly thanks BASF S.p.A. for a research grant.

REFERENCES

- (1) Hao, F.; Stoumpos, C. C.; Chang, R. P. H.; Kanatzidis, M. G., *J. Am. Chem. Soc.* **2014**, *136*, 8094-8099.
- (2) Ogomi, Y.; Morita, A.; Tsukamoto, S.; Saitho, T.; Fujikawa, N.; Shen, Q.; Toyoda, T.; Yoshino, K.; Pandey, S. S.; Ma, T.; Hayase, S., *J. Phys. Chem. Lett.* **2014**, *5*, 1004-1011.
- (3) Mosconi, E.; Umari, P.; De Angelis, F., *J. Mater. Chem. A* **2015**, *3*, 9208-9215.
- (4) Zuo, F.; Williams, S.T.; Liang, P.-W.; Chuen, C.-C.; Liao, C.-Y.; Jen, A.K.-Y., *Adv. Mater.*, **2014**, *26*, 6454-6460.
- (5) Poglitsch, A.; Weber, D., *J. Chem. Phys.*, **1987**, *87*, 6373-6378.
- (6) Swainson, I.; Chi, L.; Her, J.-H.; Cranswick, L.; Stephens, P.; Winkler, B., *Acta Cryst. B*, **2010**, *66*, 422-429.
- (7) Keller, E.; Kraemer, V.; *Acta Crystall. B*, **2006**, *62*, 411.
- (8) Kubelka, P.; Munk, F., *Zeit. Fur Techn. Physik*, **1931**, *12*, 593-601.
- (9) H.-S. Kim et al., *Scientific Reports*, **2012**, *2*, 591.
- (10) Zhang, M.; Yu, H.; Lyu, M.; Wang, Q.; Yun, J.-H.; Wang, L., *Chem. Comm.*, **2014**, *50*, 11727-11730.
- (11) Frost, J. M.; Butler, K. T.; Brivio, F.; Hendon, C. H.; van Schilfgaarde, M.; Walsh, A., *Nano Lett.*, **2014**, *14*, 2584-2590.



Diffuse reflectance spectra for the $\text{MASn}_x\text{Pb}_{1-x}\text{Br}_3$ solid solution showing a continuous gap shift towards the NIR spectral region.